J Neurooncol (2011) 104:423–438
DOI 10.1007/s11060-010-0509-x

LABORATORY INVESTIGATION - HUMAN/ANIMAL TISSUE

OLIG2 is differentially expressed in pediatric astrocytic and in ependymal neoplasms

José Javier Otero · David Rowitch · Scott Vandenberg

Received: 8 June 2010 / Accepted: 15 December 2010 / Published online: 31 December 2010

Abstract The bHLH transcription factor, OLIG2, is universally expressed in adult human gliomas and, as a major factor in the development of oligodendrocytes, is expressed at the highest levels in low-grade oligodendroglial tumors. In addition, it is functionally required for the formation of high-grade astrocytomas in a genetically relevant murine model. The pediatric gliomas have genomic profiles that are different from the corresponding adult tumors and accordingly, the expression of OLIG2 in non-oligodendroglial pediatric gliomas is not well documented within specific tumor types. In the current study, the pattern of OLIG2 expression in a spectrum of 90 non-oligodendroglial pediatric gliomas varied from very low levels in the ependymomas (cellular and tanycytic) to high levels in pilocytic astrocytoma, and in the diffuse-type astrocytic tumors (WHO grades II–IV). With dual-labeling, glioblastoma had the highest percentage of OLIG2 expressing cells that were also Ki-67 positive (mean = 16.3%) whereas pilocytic astrocytoma WHO grade I and astrocytoma WHO grade II had the lowest (0.9 and 1%, respectively); most of the Ki-67 positive cells in the diffuse-type astrocytomas (WHO grade II–III) were also OLIG2 positive (92–94%). In contrast to the various types of pediatric astrocytic tumors, all ependymomas WHO grade II, regardless of site of origin, showed at most minimal OLIG2 expression, suggesting that OLIG2 function in pediatric gliomas is cell lineage dependent.

Keywords Pediatric glioma · Pilocytic astrocytoma · Pediatric astrocytoma · Pediatric ependymoma · OLIG2

Abbreviations

bHLH	Basic helix loop helix
CBTRUS	Central Brain Tumor Registry of the United States
F-T-P Lobes	Frontal-temporal-parietal lobes of cerebral cortex
EGF	Epidermal growth factor
EGFR	Epidermal growth factor receptor
IDH1	Isocitrate dehydrogenase 1
OLIG2	Oligodendrocyte lineages transcription factor 2
PDGF	Platelet derived growth factor
PTEN	Phosphatase and tensin homologue
SEGA	Subependymal giant cell astrocytoma
WHO	World Health Organization

Introduction

Neuroepithelial tumors containing various glial lineages are the most common primary central nervous system (CNS) tumor in all age groups. Pediatric CNS tumors

Electronic supplementary material The online version of this article (doi:10.1007/s11060-010-0509-x) contains supplementary material, which is available to authorized users.

J. J. Otero (✉)
Division of Neuropathology, Department of Pathology, University of California, 505 Parnassus Avenue #M551, P.O. Box 0102, San Francisco, CA 94143, USA
e-mail: Jose.Otero@ucsfmedctr.org

D. Rowitch
Departments of Pediatrics and Neurosurgery, HHMI, University of California, San Francisco, CA, USA

S. Vandenberg
Division of Neuropathology, Department of Pathology, University of California, San Diego, CA, USA

constitute a large group of solid neoplasms that arise within the first two decades and are the second most common malignancy in children, second only to leukemia [1]. In pediatric patients, gliomas account for 45–56% of all CNS tumors and 74–81% of all malignant CNS tumors [2]. Within this group, the non-oligodendroglial gliomas are a leading cause of solid tumor-related morbidity and mortality in children. The development of effective therapies for these tumors has been limited, in part due to a limited understanding of the genetic alterations responsible for their development and progression.

Several lines of evidence suggest that the activity of OLIG2 provides a mechanistic link between growth of malignant glioma progenitors and neural stem cells. First, a subpopulation of type B and type C progenitor cells in the adult rodent brain express OLIG2 [3–5]. Second, exposure to glioma relevant mitogens such as EGF or PDGF [6] stimulates proliferation of OLIG2+ rapidly dividing "type C" transit amplifying cells and glioma-like growths. All adult malignant gliomas, irrespective of grade, express OLIG2 in at least a fraction of the malignant cell population [7, 8]. Third, OLIG2 function is required for tumorigenesis in a genetically relevant mouse model of adult human gliomas that commonly show activation of EGF signaling and mutation of the tumor suppressor INK4A/ARF [9].

The pediatric gliomas share histopathologic similarities with their corresponding adult counterparts, even though they do not have the same signature genetic mutations, such as genomic alterations in the EGFR, PTEN, and TP53 [10–15]. Although TP53 mutations are present in several groups of pediatric gliomas, the frequent genetic alterations detected in adult WHO grade II-IV astrocytomas, including IDH1 mutations, are identified at significantly lower frequencies in pediatric gliomas [1, 16–19]. Recently, several studies have shown that a majority of pilocytic astrocytomas in both pediatric and adult patients harbor 7q34 duplications, which result in gene fusions between KIAA1549 and BRAF with the concomitant expression of KIAA1549:BRAF fusion transcripts [20, 21]. In addition, a number of pediatric infiltrating gliomas (WHO grades II-IV) also appear to harbor an activating BRAFV600E mutation that may also occur with homozygous deletions in the *CDKN2A* gene [22]. The question of the prevalence of OLIG2 expression in the non-oligodendroglial pediatric gliomas is relevant in view of the genomic distinctions within pediatric astrocytic tumors and distinct biological features of these tumors in contrast to their adult counterparts.

Materials and methods

Patient material selection

Pediatric brain tumor cases from 1990 to 2008 were retrieved from the UCSF Pathology archives. Neurosurgical patients below 20 years of age with a primary brain tumor of glial origin were included in this study, but cases of recurrent tumors were grouped separately from primary, newly diagnosed tumors undergoing first resection. A total of 90 pediatric cases were retrieved from the archives that met these criteria (see Tables 1, 2; Fig. 1 for further information). Many of these cases had been originally

Table 1 OLIG2 expression in primary CNS tumors

Diagnosis	Average age (years)	M/F	Mean OLIG2 score	SD
Glioblastoma, WHO grade IV	8.7	2M/4F	3	0
Anaplastic astrocytoma, WHO III	7.6	8M/5F	2.2	0.9
Recurrent anaplastic astrocytoma, WHO III	17	2M/0F	3	0
Astrocytoma, WHO II	10.6	9M/4F	2.6	0.8
Recurrent astrocytoma, WHO II	11.8	2M/2F	1.4	1.1
Pilocytic astrocytoma, WHO I	6.9	13M/19F	3	0.18
Recurrent pilocytic astrocytoma, WHO I	10.5	2M/0F	2.5	0.7
Ependymoma, WHO II	10.1	4M/4F	0	0
Recurrent ependymoma, WHO II	7.5	1M/1F	0.4	0.5
Anaplastic ependymoma, WHO III	7.8	3M/1F	0.25	0.5
Myxopapillary ependymoma	15	1M/1F	1.5	2.1
SEGA	6	1M/1F	0	0

Pediatric brain tumors were scored for OLIG2 expression by immunohistochemistry. Ependymomas (including one tanycytic variant) showed no OLIG2 staining, whereas one myxopapillary ependymomas showed strong OLIG2 expression. WHO II and pilocytic astrocytomas showed decreased OLIG2 staining after treatment, but this value is not statistically significant by ANOVA. Recurrent neoplasms, i.e., a treated neoplasm

y Years, *M/F* number male patients/number female patients, *ST error* standard error of the mean, *WHO* world health organization, *roman numerals* WHO grade

Table 2 CNS tumors showing statistically significant OLIG2 expression

Tumor 1	Tumor 2	*P* value
Anaplastic ependymoma, WHO III	Anaplastic astrocytoma, WHO III	$<1 \times 10^{-5}$
Ependymoma, WHO II	Anaplastic astrocytoma, WHO III	$<1 \times 10^{-5}$
Pilocytic astrocytoma, WHO I	Anaplastic astrocytoma, WHO III	0.017
Recurrent ependymoma, WHO II	Anaplastic astrocytoma, WHO III	0.0058
SEGA, WHO I	Anaplastic astrocytoma, WHO III	3×10^{-4}
Astrocytoma, WHO II	Anaplastic ependymoma, WHO III	$<1 \times 10^{-5}$
Glioblastoma, WHO IV	Anaplastic ependymoma, WHO III	$<1 \times 10^{-5}$
Pilocytic astrocytoma, WHO I	Anaplastic ependymoma, WHO III	$<1 \times 10^{-5}$
Recurrent anaplastic astrocytoma, WHO III	Anaplastic ependymoma, WHO III	6.6×10^{-5}
Recurrent pilocytic astrocytoma, WHO I	Anaplastic ependymoma, WHO III	0.0024
Ependymoma, WHO II	Astrocytoma, WHO II	$<1 \times 10^{-5}$
SEGA, WHO I	Astrocytoma, WHO II	$<1 \times 10^{-5}$
Glioblastoma, WHO IV	Ependymoma, WHO II	$<1 \times 10^{-5}$
Pilocytic astrocytoma, WHO I	Ependymoma, WHO II	$<1 \times 10^{-5}$
Recurrent anaplastic astrocytoma, WHO III	Ependymoma, WHO II	$<1 \times 10^{-5}$
Recurrent astrocytoma, WHO II	Ependymoma, WHO II	0.017
Recurrent pilocytic astrocytoma, WHO I	Ependymoma, WHO II	7.2×10^{-5}
Recurrent astrocytoma, WHO II	Glioblastoma, WHO IV	0.0039
Recurrent ependymoma, WHO II	Glioblastoma, WHO IV	5.1×10^{-5}
SEGA, WHO I	Glioblastoma, WHO IV	$<1 \times 10^{-5}$
Recurrent astrocytoma, WHO II	Pilocytic astrocytoma, WHO I	$<1 \times 10^{-5}$
Recurrent ependymoma, WHO II	Pilocytic astrocytoma, WHO I	$<1 \times 10^{-5}$
SEGA, WHO I	Pilocytic astrocytoma, WHO I	$<1 \times 10^{-5}$
Recurrent ependymoma, WHO II	Pilocytic astrocytoma, WHO I	$<1 \times 10^{-5}$
SEGA, WHO I	Recurrent anaplastic astrocytoma, WHO III	2.1×10^{-3}
Recurrent pilocytic astrocytoma, WHO I	Recurrent ependymoma, WHO II	0.031

ANOVA/Tukey HSD test were performed to test which tumor comparisons showed a statistically significant difference in OLIG2 expression. Only tumor comparisons with statistical significance are listed

P adjusted probability calculated by Tukey HSD test

diagnosed using non-WHO grading criteria, and therefore a thorough review of all cases was carried out jointly by the authors (JO and SV) to assign accurate 2007 WHO grade for each case. Both authors agreed with the final diagnosis and WHO grade. For comparison to the pediatric ependyomomas, 10 cases of adult ependymoma were analyzed: 3 myxopapillary ependymoma, WHO grade I (average age = 32 years, two female, one male); 6 ependymoma, WHO grade II (average age = 33.7 years, three male, three female); 1 anaplastic ependymoma, WHO grade III (54 year old male). Hematoxylin and Eosin (H&E) stained sections were reviewed by the authors (SRV and JJO) for diagnostic confirmation and to select appropriate tissue blocks for subsequent OLIG2 immunoperoxidase staining. Specifically, one H&E stained section and one OLIG2 stained section was evaluated. During review of OLIG2 stained sections, access to the original pathological diagnosis was permitted. Full concordance in diagnosis and OLIG2 expression was established for all cases studied. Selection of histologic sections for immunoperoxidase stains required the following criteria: (1) the section had to be representative of the final diagnosis, (2) only tissue that was formalin fixed while fresh and paraffin embedded was used (i.e., remnants from previously frozen tissue were excluded from the study), and (3) sufficient material had to be present for evaluation (greater than or equal to 0.01 cm^2 of tissue per slide and multiple blocks if possible). The definition of brainstem included midbrain, pons, and medulla. The definition of deep gray matter used in this study includes tumors arising in hypothalamus, thalamus, basal ganglia, and striatum.

Immunohistochemistry techniques

All tissue was routinely fixed in either phosphate buffered 4% formalin or Zn-4% Formalin, dehydrated by graded ethanol washes and embedded in wax (Paraplast Plus, McCormick Scientific) using routine techniques. All sections were cut at 5 μm thickness and mounted upon *Superfrost/Plus* slides (Fisher Scientific). Antibodies were obtained from the following sources and used at the following dilutions and incubation times/temperatures: (1) OLIG2 rabbit polyclonal antibody DF308 (From lab stocks, [23]): 1:50, 32 min at 37°; (2) Anti Ki-67 rabbit polyclonal (Anti-Ki-67(30-9), Ventana Medical Systems, Tucson, AZ) 2 μg/ml, 32 min at 37°. Epitope retrieval for

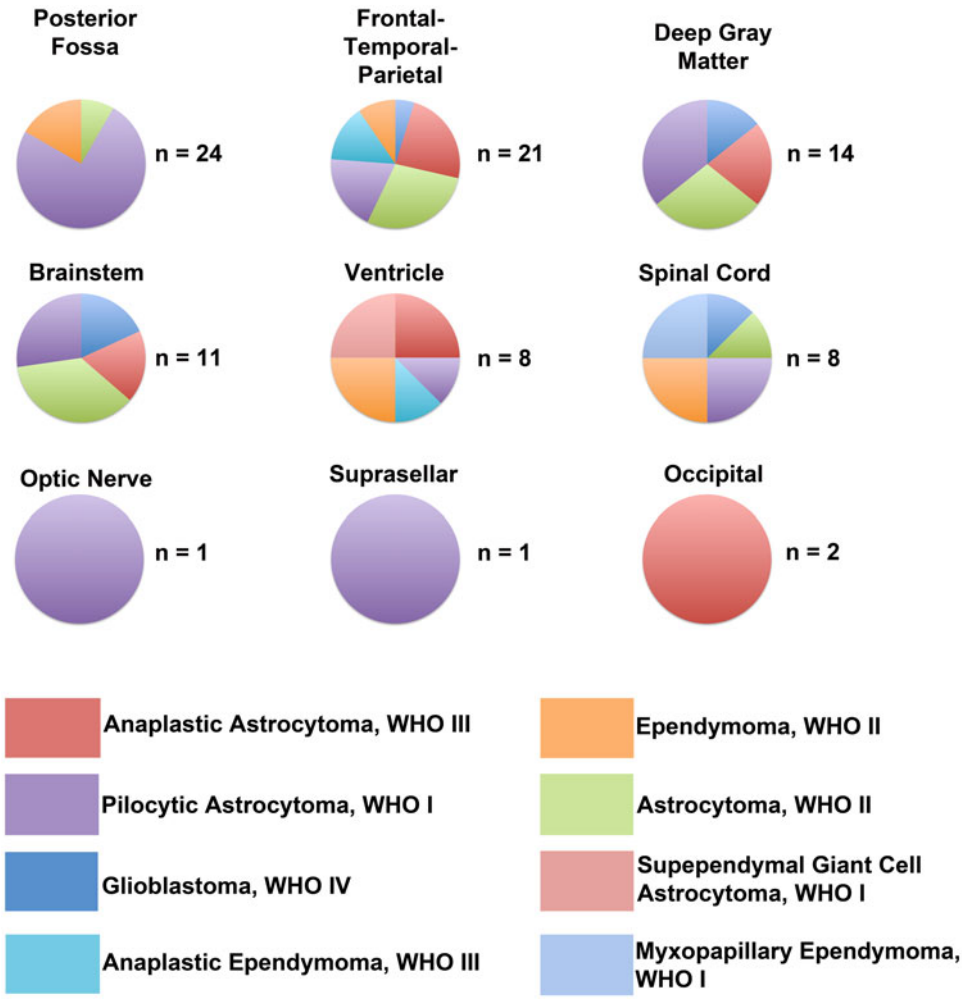

Fig. 1 Distribution of primary brain tumor per anatomical site in this patient cohort. The distribution of brain tumors per anatomical site is illustrated in pie charts. Below the pie chart is its anatomical site; to the right of the pie chart is the total number of cases (*n*) in that site. The largest proportions of tumors in the respective sites were: occipital lobe -> anaplastic astrocytoma (2 of 2 total cases); frontal/temporal/parietal cortex ->astrocytoma WHO II (6 of 21 total cases); posterior fossa ->pilocytic astrocytoma (18 of 24 total cases); deep gray matter ->pilocytic astrocytoma (5 of 14 total cases); brainstem ->astrocytoma, WHO II (4 of 11 cases); ventricle/periventricular -> anaplastic astrocytoma WHO III, SEGA WHO I, ependymoma (each were 2 of 8 total cases); spinal cord ->pilocytic astrocytoma, ependymoma WHO II, myxopapillary ependymoma (each were 2 of 8 total cases); optic nerve ->anaplastic astrocytoma WHO III (1 of 1 total case); suprasellar ->pilocytic astrocytoma (1 of 1 total case)

OLIG2 was performed in Tris buffer pH 8 at 90° for 60 min, and for Ki-67 performed in Tris buffer pH 8 at 90° for 30 min. All immunohistochemistry was performed on the Ventana Medical Systems Benchmark XT using the *Ultraview* (multimer) detection system. Negative staining in endothelial cells was used as an internal negative control. Dual labeling for OLIG2 and Ki-67 was also performed using the Ventana Medical Systems Benchmark XT using Ultraview DAB (OLIG2) and RED (Ki-67) chromogens.

Immunohistochemistry scoring

Patient "cases" were defined as all surgical biopsies/resection tissue from a single surgical procedure and included all tissue submitted to pathology. All cases were reviewed and scored independently by two of the authors (Drs. Vandenberg and Otero) for the OLIG2 immunoperoxidase stain. This antibody has been validated in other studies and is immunoreactive in various tumor cells of adult gliomas [23]. A corresponding H&E stained section was also available to confirm the OLIG2 immunoreactivity in tumor cell nuclei. Microvascular cells were internal negative controls. Cases were scored for OLIG2 tumor expression as follows: score 0 corresponded to no OLIG2 staining in the tumor cells; score 1 corresponded to OLIG2 staining in 1–25% of tumor cells; score 2 corresponded to OLIG2 staining in 26–75% of tumor cells; score 3 corresponded to OLIG2 staining in more than 75% of tumor cells. The scoring was done independently by two of the authors (Drs. Vandenberg and Otero) with similar results. Images shown in Figs. 2, 3, 4 and 5 demonstrate representative fields of selected cases. For cases with multiple sections/case, the score of all of the sections were averaged into a final "case score." The results from all of the cases of a particular tumor type (cases were categorized by diagnosis and tumor site in Tables 1, 2 and 3) are derived from means of the score for each case (this includes averages from cases with multiple sections/case as well as the score from cases with one section/case).

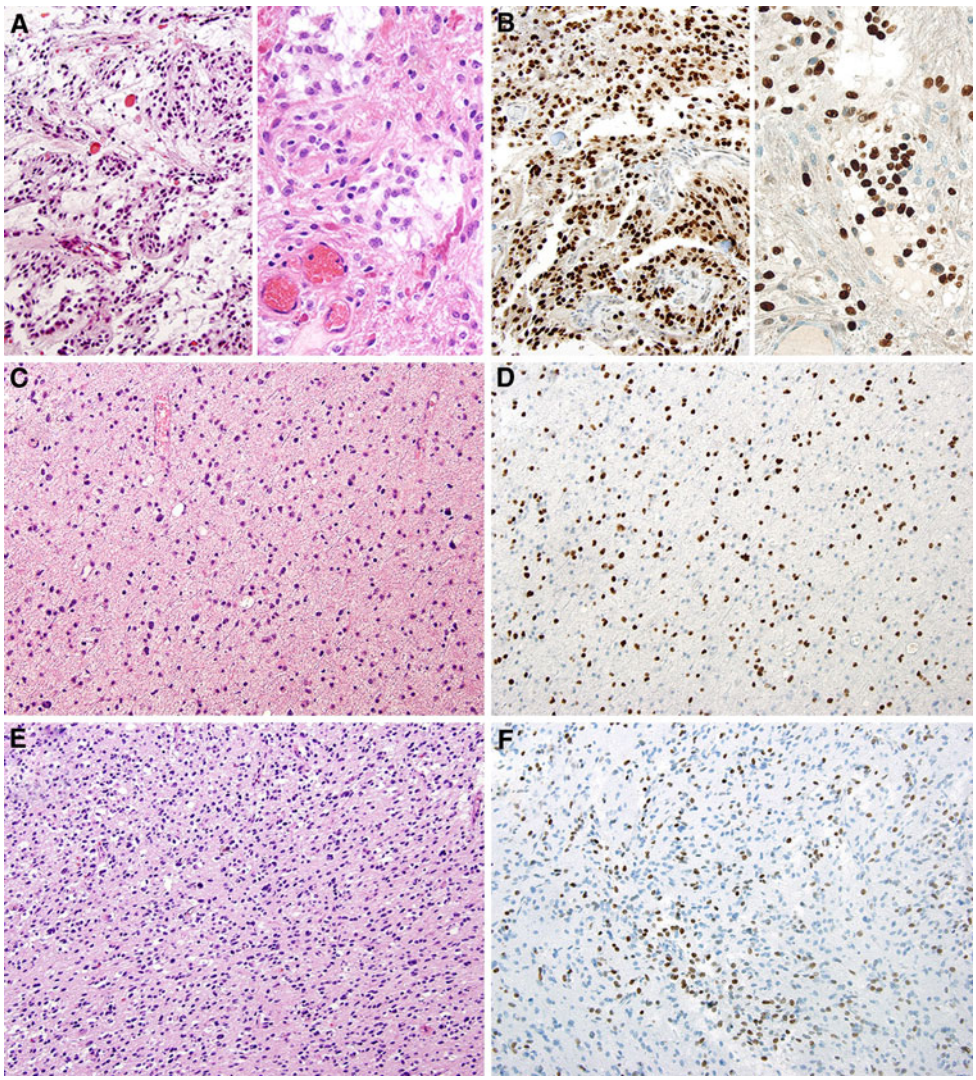

Fig. 2 OLIG2 Immunoreactivity in pilocytic astrocytomas (WHO Grade I) and diffuse-type astrocytomas (WHO Grade II–III). Representative images of the following tumor types illustrate the most common expression patterns. Pilocytic astrocytoma: (**a**) Hematoxylin and eosin. (**b**) OLIG immunohistochemistry. Diffuse-type astrocytoma, WHO Grade II: (**c**) Hematoxylin and eosin. (**d**) OLIG immunohistochemistry. Diffuse-type astrocytoma, WHO Grade III: (**e**) Hematoxylin and eosin. (**f**) OLIG immunohistochemistry. **a** and **b** are split with low magnification images on the left and high magnification images on the right. Most pilocytic astrocytomas showed near universal, diffuse OLIG2 expression

Dual-label OLIG2-Ki67 immunohistochemistry

Selected cases that were dual-immunolabeled for OLIG2 and MIB-1 included pilocytic astrocytoma, infiltrating astrocytoma WHO grade II, anaplastic astrocytoma WHO grade III, and one glioblastoma multiforme. Staining was performed with hematoxylin counterstain to verify the labeled tumor cells and to exclude labeled inflammatory and/or vascular nuclei and without hematoxylin counterstain to optimize the quantitative detection of dual-labeled cells. A replicate slide without hematoxylin counterstain was used for all quantifications as this facilitated detection of dual labeled cells. Quantification was performed using the technique for Ki-67 labeling indexes in gliomas used by Colman and colleagues [24]. Briefly, digital pictures of the tissue samples were taken and cell counts were determined using the open source ImageJ cell counter software (http://rsbweb.nih.gov/ij/). Three of five infiltrating astrocytoma WHO grade II and one in six anaplastic astrocytoma WHO grade III had fewer than 1000 tumor cell nuclei per slide. All other cases had over 1000 cell nuclei analyzed. Nuclei of Ki67+/OLIG2-cells were bright pink-red color whereas Ki67+/OLIG2+ were dark red-brown in this dual color reaction.

Genetic analysis of BRAF in pediatric gliomas

Select cases had been evaluated for BRAF alterations, including BRAFV600E missense mutations and KIAA1549-BRAF fusion transcripts. BRAF analysis of these cases was reported previously by Schiffmen et al. [22]. To evaluate statistical correlations, Fisher Exact Test was performed using R v2.11.1, an open source statistical framework run on MAC OS Terminal (http://cran.r-project.org/).

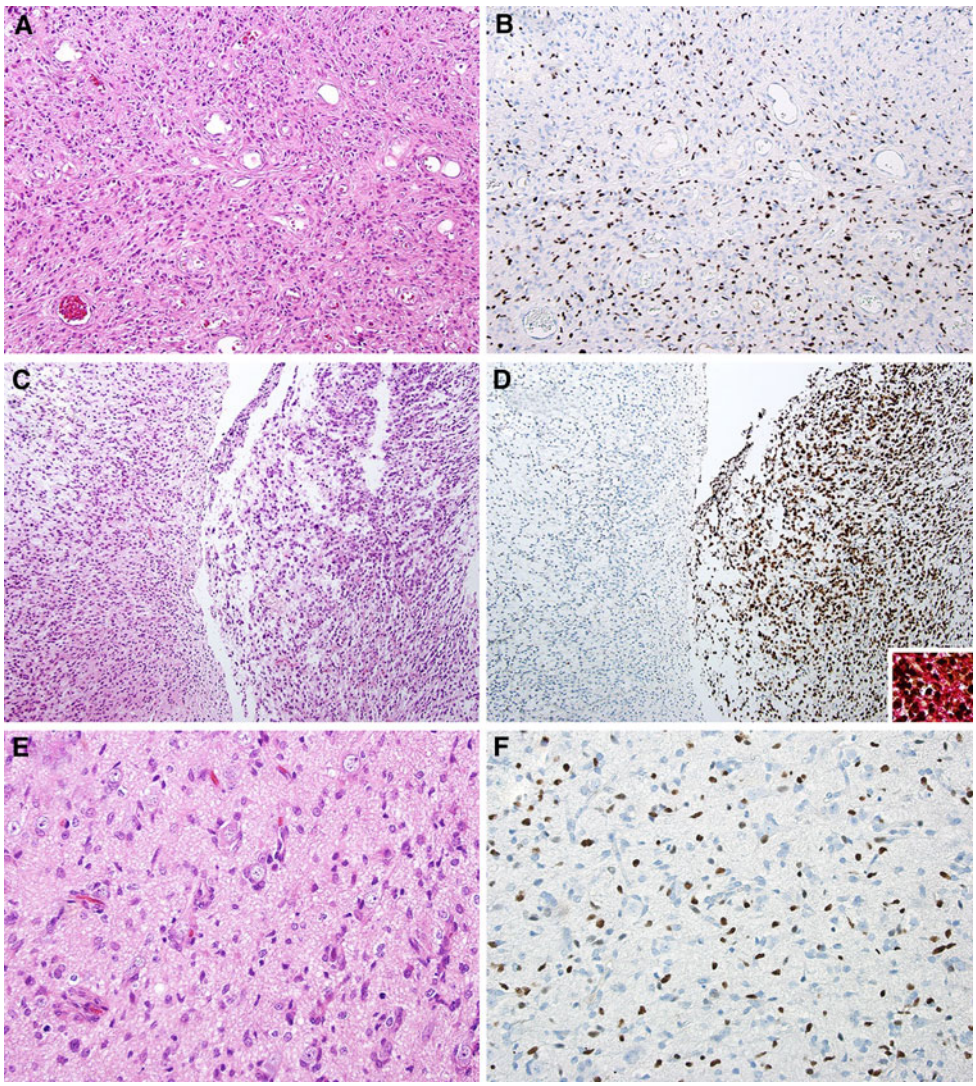

Fig. 3 Patterns of OLIG2 Immunoreactivity in Pediatric Glioblastoma, WHO grade IV. Three examples of Glioblastoma (WHO grade IV) are illustrated to demonstrate distinct patterns of OLIG2 expression. **a, c, e** show H&E stained sections and **c**, **d**, and **f** illustrate OLIG2 immunohistochemistry. The first case (17 year old male with spinal cord GBM, **a**, and **b**, demonstrates widespread OLIG2 expression in tumor cells. Another pattern noted is illustrated in **c** and **d** (8 year old female with a right thalamic GBM). Note the biphasic pattern of OLIG2 expression in this tumor. The more primitive cellular OLIG2+ population was GFAP immunoreactive (**d** *inset*, dual label OLIG2 brown-GFAP red). **e** and **f** (9 year old male with temporal lobe GBM) shows the typical perineuronal and perivascular invasive pattern at the edge of a GBM. Note that the OLIG2 expressing cells at the infiltrative edge of the tumor do not have a specific distribution pattern

In silico analysis of ependymoma and juvenile pilocytic astrocytoma Affymetrix microarray data

The ependymoma microarray dataset performed by Johnson et al. [25], the juvenile pilocytic astrocytoma microarray dataset performed by Sharma et al. [26], and the pediatric high grade glioma dataset performed by Paugh et al. [11] were downloaded from the Gene Expression Omnibus (http://www.ncbi.nlm.nih.gov/geo/). The ependymoma and pilocytic astrocytoma datasets had been performed using the Affymetrix HG-U133 plus 2 GeneChip mircroarray using similar techniques. Ependymoma GEO accession number is GSE21687 and the pilocytic astrocytoma GEO accession number is GSE5675. The high grade glioma dataset GEO accession number is GSE19578. Evaluation of the pediatric high grade glioma dataset performed by Paugh et al. [11] was not directly compared to the pilocytic astrocytoma and ependymoma data as the test design was performed in a distinct fashion. This high grade dataset is composed of single microarrays from multiple patients. In addition, quality control analysis showed significant differences in average probe pm intensities as well as occasional arrays with RNA degradation that was significantly different from the ependymoma and pilocytic astrocytoma datasets. The ependymoma and pilocytic astrocytoma datasets were composed of triplicates, resulting in three .cel files in both the ependymoma and pilocytic astrocytoma arrays. The .cel files were read into the R v2.11.1 using Bioconductor's *affy* library package (http://www.bioconductor.org/), an open source R library package routinely used for the analysis of microarray data [27]. An *Affybatch* object was instantiated containing all files with the probe level data (three .cel files from the ependymoma dataset and three .cel from the pilocytic astrocytoma dataset). In the case of the high grade glioma dataset, .cel files corresponding to glioblastoma patients were used

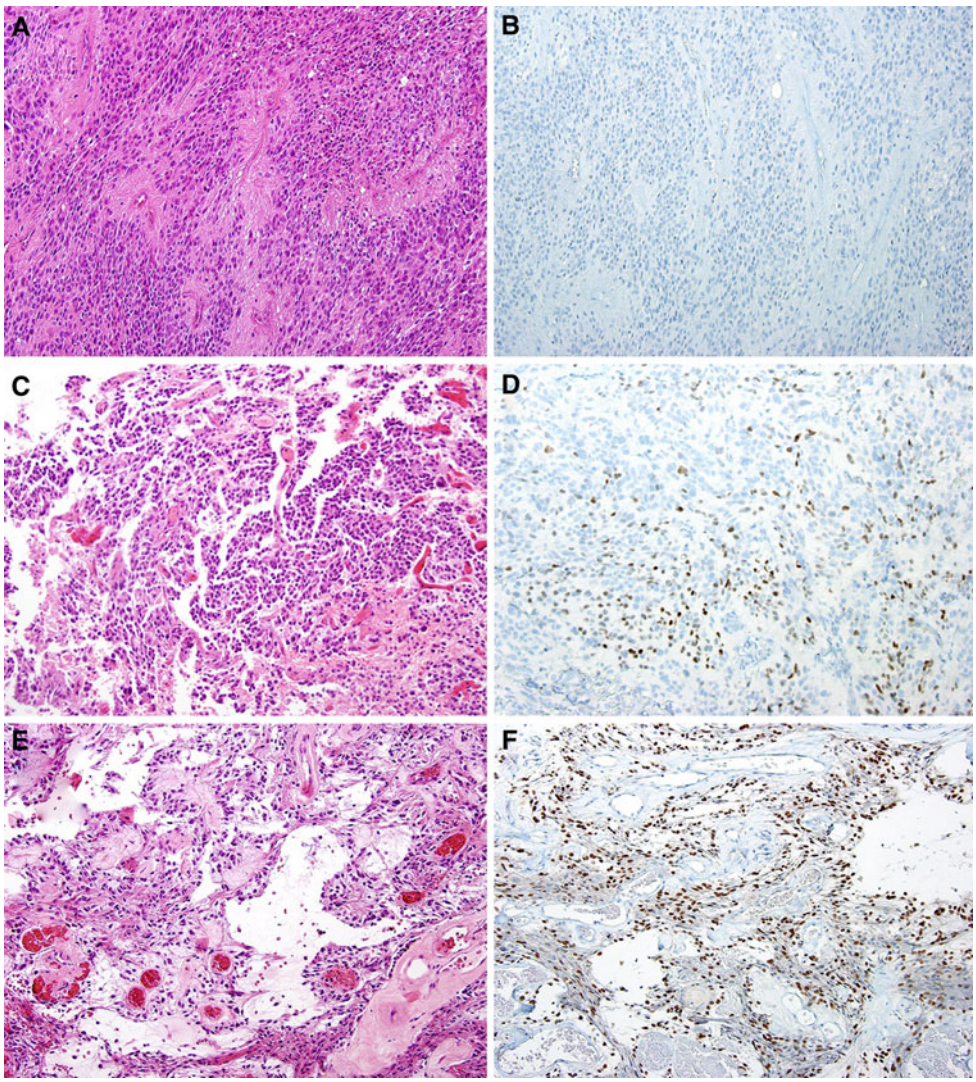

Fig. 4 OLIG2 Immunohistochemistry in pediatric ependymomas. H&E stained sections for pediatric ependymomas are illustrated on the *left panels* with the corresponding OLIG2 immunohistochemistry on the *right*. The majority of ependymomas showed no staining for OLIG2 as shown in **b**. One recurrent ependymoma (8 year old male with a posterior fossa mass) showed focal OLIG2 positive tumor cells (**d**). Included in the study cohort was one patient with myxopapillary ependymoma that shows intense and diffuse OLIG2 staining (**f**)

to instantiate an *Affybatch* object composed of 28 .cel files. Background correction and normalization was performed using Bioconductor's *expresso* function (settings used: normalize.method = "qspline", bgcorrect.method = "rma" [28–30], pmcorrect.method = "pmonly", summary.method = "liwong" [31]). The expression measures were derived by use of robust multiarray average (RMA). Expression measures were then written to a .txt or .csv file for further analysis. To determine differential gene expression between the ependymoma and pilocytic astrocytoma microarrays, RMA correction of the *Affybatch* object containing all .cel files was performed and evaluated with the *lmFIt* and *topTable* functions of Bioconductor's *limma* package [32]. Quality control analysis of the microarray data was performed using Bioconductor's *QCReport* package (http://bioconductor.org/packages/2.6/bioc/html/affyQCReport.html); quality control data for the two array studies derived from *QCReport* is shown in Supplementary Fig. 1.

Conversion of affymetrix gene ID to gene names was done with the David Gene ID conversion tool (http://david.abcc.ncifcrf.gov/) [33, 34]. Table 6 lists known genes with the most significant differential expression as determined by the *lmFit* function of Bioconductor's *limma* package. Log fold change (logFC) and statistical analysis of differential gene expression in Table 6 was performed by the *lmFit* function. Table 7 lists the *expresso* derived RMA expression measures of the ependymoma and pilocytic astrocytoma arrays of genes known to be expressed in stem cell, astrocytic, oligodendroglial, and ependymal cell lineage of non-neoplastic brain. RMA expression measures of E-box containing genes that showed differential expression in OLIG2 null versus wild-type neurospheres as described by Ligon et al. [9] were evaluated using similar techniques. Paired, two-tailed student's *t*-test was used to calculate *P*-values of the expression measures listed in Tables 6 and 7.

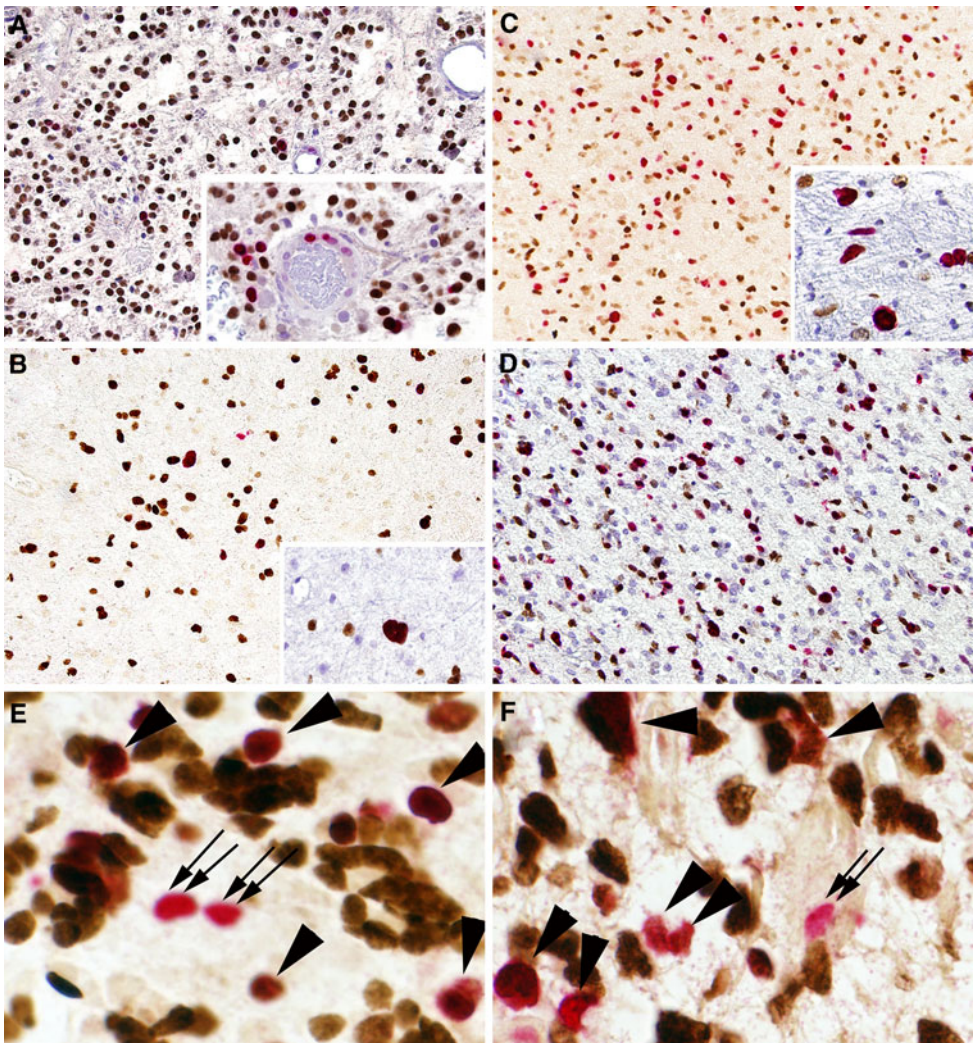

Fig. 5 OLIG2/Ki-67 dual immunohistochemistry of pediatric gliomas. Select cases of pediatric gliomas were dual immunolabeled for OLIG2 (DAB chromogen) and Ki-67 (RED chromogen). **a** Pilocytic astrocytoma, WHO Grade I; (**b**) Diffuse-type astrocytoma, WHO grade II; (**c**) Anaplastic astrocytoma, WHO grade III; (**d**) Glioblastoma, WHO grade IV. High magnification views of dual labeled anaplastic astrocytoma (**e**) and glioblastoma WHO IV (**f**) are illustrated to highlight the differences between OLIG2+/Ki67+ cells and OLIG2-/Ki67+ cells. *Double arrows* in **e** and **f** are OLIG2-/Ki67+ cells and large arrowheads are OLIG2+/Ki67+ cells. The majority of Ki67 positive cells are also OLIG2 positive

Results

Distribution of pediatric brain tumor cases

As shown in Table 1, the most common brain tumor in the patient cohort was the pilocytic astrocytoma, accounting for 36% of the tumors studied. However, infiltrating astrocytomas (i.e., all astrocytoma WHO II, III, and IV) as a group exceeded the number of pilocytic astrocytoma cases, accounting for 42% of the cases studied. Astrocytomas are therefore slightly over represented in this cohort compared to that reported in the CBTRUS, in which pilocytic astrocytomas (WHO grade I) comprise 14–20% of tumors and infiltrating astrocytomas range from 11–15% of tumors [2].

Anatomical site of the tumors is listed in Table 3, and the distributions of tumor type per anatomical site is illustrated in Fig. 1. The most common tumor site was the posterior fossa (26.7%), followed by the cerebral hemispheres (in toto, 25.6%). As the specific proportion of cortical based and cerebellar based brain tumors are slightly increased relative to the CBTRUS population (18 and 16%, respectively), these tumor sites are overrepresented in this cohort. Infiltrating astrocytomas (WHO Grades II–IV) accounted for the majority of the tumors arising in the cerebral hemispheres, while the majority of posterior fossa tumors were pilocytic astrocytomas (Fig. 1).

Distribution of OLIG2 expression in pediatric tumors

All astrocytic tumors, including all pilocytic astrocytomas (WHO Grade I) and the diffuse-type astrocytomas (WHO Grades II–IV) showed diffuse OLIG2 expression (Table 1). The glioblastomas and the pilocytic astrocytomas had the highest mean OLIG2 score, followed by the diffuse-type infiltrating astrocytomas WHO grade II–III. The primary ependymomas (including anaplastic ependymoma, WHO grade III) and two subependymal giant cell astrocytoma were noteworthy for the absence of OLIG2+ cells. Evaluation of adult ependymomas also showed a near absence

Table 3 OLIG2 expression in primary brain tumor anatomical site

Tumor site	*n*	Ave. age	M/F	Mean OLIG2 score	SD
Optic nerve	1	3	1M/0F	3	N/A
Suprasellar zone	1	3	0M/1F	3	N/A
Deep cerebral gray matter	14	6.1	8M/6F	2.7	0.6
Posterior fossa/cerebellum	24	8.3	11M/13F	2.4	1
Brainstem	11	7.4	6M/5F	2.5	0.82
Spinal cord	8	13.1	4M/4F	2	1.4
Frontal-temporal-parietal lobes	21	9.9	13M/8F	1.8	1.2
Occipital lobes	2	6	2M/0F	1	0
Ventricular system	8	9.9	4M/4F	0.6	1.1

Primary brain tumors were analyzed for OLIG2 expression by immunohistochemistry. The results of the anatomical sites are shown here. Tumors arising in the ventricular system showed markedly decreased OLIG2 expression

n total number of cases, *y* years, *M/F* number male patients/number female patients, *ST dev* standard deviation, *Occipital* all tumors arising in the occipital lobe, *Subcortical Grey matter* all tumors arising in thalamus, hypothalamus, and basal ganglia nuclei

of OLIG2+ tumor cells (i.e., non-recurrent adult ependymoma WHO II and non-recurrent pediatric ependymoma WHO II were OLIG2 score = 0). The recurrent anaplastic astrocytomas (WHO grade III) and the recurrent cellular ependymomas tended to have a higher number of OLIG2+ cells in comparison to the corresponding primary tumors whereas the recurrent lower grade astrocytic tumors (WHO grade I and II) had much lower numbers of OLIG2+ cells. Analysis of variance (ANOVA) was performed to test the significant differences between OLIG2 expressions amongst the tumor types. The *P*-values of statistically significant tumor comparisons derived from intergroup comparison (performed by ANOVA/Tukey HSD test) are listed in Table 2. In summary, OLIG2 expression in SEGA and ependymomas were significantly lower than the astrocytic neoplasms.

Figure 2 shows representative fields of the astrocytic tumors: pilocytic astrocytoma, infiltrating astrocytoma WHO grade II–III. Many of the pilocytic astrocytoma cases showed near universal, diffuse OLIG2 expression, as illustrated in Fig. 2b, left panel. Glioblastoma, as a group showed intense OLIG2 expression, but the distribution patterns of the immunoreactive cells varied. The most common pattern was a relatively diffuse expression in single cells or small cell clusters as shown in Fig. 3b. One glioblastoma arising in the thalamus, illustrated in Fig. 3d, demonstrated a biphasic pattern of OLIG2 expression with majority of the OLIG2 immunoreactive nuclei in the more poorly differentiated cells that were distributed in highly cellular zones while the more differentiated astrocytic phenotypes were OLIG2 negative. These poorly differentiated, OLIG2+ cells were also immunoreactive for GFAP (Fig. 3d, inset). When an infiltrating edge of the glioblastomas was available for analysis, OLIG2 positive tumor cells were present in the populations of tumor cells infiltrating the surrounding brain; however, in contrast to the overall tendency for localization of the tumor cells in perineuronal and perivascular zones, OLIG2+ cells did not show a preferential perineuronal satelitosis or perivascular structuring (Figs. 2e, f).

A total of 16 pediatric ependymomas were tested for OLIG2 expression. Representative photographs of OLIG2 stained ependymomas are shown in Fig. 3. The majority of cases (13 of 16) showed no significant OLIG2 expression (score = 0). One case of myxopapillary ependymoma showed a diffuse, strong expression of OLIG2. A second case of myxopapillary ependymoma showed no OLIG2 expression. Discrete zones of OLIG2+ cells were present in one case of recurrent cellular ependymoma in an 8-year old boy (see Fig. 3d) and in one case of a 17-year old boy with a fourth ventricular anaplastic ependymoma, WHO III (data not shown). The OLIG2 staining pattern in the recurrent pediatric ependymoma is more typical of that described in adult ependymomas [23]. Taken together, 18.8% of pediatric ependymoma cases showed at least some OLIG2 expression, a result similar to that reported by other investigators [35–37]. Comparison of OLIG2 expression in adult ependymomas showed similar results to the pediatric ependymomas (mean OLIG2 score = 0). No adult myxopapillary ependymomas (0 of 3 total cases) showed significant OLIG2 expression.

Tumor type and anatomic site affecting OLIG2 expression

Although the level of OLIG2 expression appeared to vary according to tumor site (Table 3), this trend usually resulted from the disparity of specific tumor types that were associated with particular anatomic zones. However, the anaplastic astrocytomas that arose in the occipital lobes had low OLIG2 expression compared to other sites, and regardless of tumor type, tumors arising in the deep supratentorial midline structures (suprasellar, optic nerve, thalamus) typically had high levels of OLIG2 expression. The anatomical site that showed the highest OLIG2 expression was the deep cerebral gray matter (average OLIG2 score of 2.7). The anatomical sites with the lowest OLIG2 expression were intraventricular tumors (average OLIG2 score = 0.66). Intraventricular tumors were chiefly composed of low OLIG2 expressing tumors such as SEGA and ependymoma. Tumors arising in the frontal/temporal/parietal cerebral cortex show a large variation in OLIG2 expression (standard deviation of OLIG2 score = 1.2).

Table 4 OLIG2 and Ki67 dual quantifications in pediatric human gliomas

Case number	Diagnosis	Percentage of OLIG2+ cells that are also Ki67+	Percentage of Ki67+ cells that are also OLIG2 positive
1	Pilocytic astrocytoma, WHO grade I	1.6	100
2	Pilocytic astrocytoma, WHO grade I	0	*
3	Pilocytic astrocytoma, WHO grade I	0	*
4	Pilocytic astrocytoma, WHO grade I	0.6	88.9
5	Pilocytic astrocytoma, WHO grade I	0.1	100
6	Pilocytic astrocytoma, WHO grade I	0	*
7	Pilocytic astrocytoma, WHO grade I	5	80.3
8	Pilocytic astrocytoma, WHO grade I	0	*
9	Pilocytic astrocytoma, WHO grade I	0.5	54.5
	Mean of pilocytic astrocytoma	0.9 (SEM = 0.5)	85.0 (SEM = 6.2)
1	Astrocytoma, WHO grade II	0.1	100
2	Astrocytoma, WHO grade II	0.5	100
3	Astrocytoma, WHO grade II	1.7	100
4	Astrocytoma, WHO grade II	2	71.4
5	Astrocytoma, WHO grade II	0.9	100
	Mean of astrocytoma, grade II	1.0 (SEM = 0.3)	94.3 (SEM = 5.7)
1	Anaplastic astro, WHO grade III	0.2	100
2	Anaplastic astro, WHO grade III	12.4	92.9
3	Anaplastic astro, WHO grade III	2.4	86.2
4	Anaplastic astro, WHO grade III	1	94.1
	Mean anaplastic astrocytoma	4.9 (SEM = 2.8)	93.3 (SEM = 2.8)
1	Glioblastoma Multiforme WHO grade IV	9.2	80.4
2	Glioblastoma Multiforme WHO grade IV	23.6	88.7
	Mean of glioblastoma	16.3 (SEM = 7.2)	84.5 (SEM = 4.1)

Dual labeling indexes were determined for select tumors (see methods). The percentage of OLIG2-positive cells that are also Ki67-positive cells is calculated by dividing the number of double positive cells by the total number of OLIG2-positive cells, or %[(Ki67+ OLIG2+)/OLIG2+]. The percentage of Ki67-positive cells that are also OLIG2 positive cells is calculated by taking the number of double positive cells divided by the total number of Ki67 positive cells, or %[(Ki67+/OLIG2+)/Ki67+]. Statistical analysis by ANOVA discloses no statistical significance between the data sets presented. Cases with * showed no Ki67+ cells in the tissue section

Most astrocytic neoplasms arising in frontal/temporal/parietal cerebral cortex showed diffuse levels of OLIG2 expression; however, three cases of anaplastic ependymoma, WHO III showed low OLIG2 expression (OLIG2 score = 0), which accounts for the large variability (standard deviation = 1.2). Statistical analysis by ANOVA and Tukey HSD test demonstrates that only ventricle-brainstem, ventricle-deep deep gray matter, and ventricle-posterior fossa comparisons were statistically significant ($P = 0.005$, 0.0009, 0.002, respectively). OLIG2 expression differences between all other sites were not statistically significant (in all instances, $P > 0.05$).

Cellular proliferation and OLIG2+ expression

OLIG2 regulates replication competence in a genetically relevant murine model [9]. To test if proliferating cells were OLIG2 positive, the proportion of Ki67+ cells that were also OLIG2+ were determined in selected cases of pilocytic astrocytoma, infiltrating astrocytoma WHO grade II, anaplastic astrocytoma WHO grade III, glioblastoma WHO grade IV, and ependymoma WHO grade II. Dual labeling immunohistochemistry for OLIG2 and Ki-67 was performed without a hematoxylin counterstain. Hence, to obtain a surrogate Ki67 labeling index in the cases examined, the proportion of OLIG2+ cells that are also Ki67+ was determined. Results for astrocytoma are listed in Table 4, and examples of dual labeling are shown in Fig. 5. Glioblastoma had the highest percentage of OLIG2 expressing cells that were also Ki-67 positive (i.e., mean (number of OLIG2+ Ki67+ cells)/total Ki67+ cells = 16.3%) and also the highest subpopulation of OLIG2− cells within the fraction of proliferating cells (i.e., mean (number of OLIG2-Ki67+ cells)/total Ki67+ cells = 15.5%). Most of the proliferating (Ki-67 positive) cells in the diffuse-type astrocytomas (WHO grade II-III)

Table 5 OLIG2 expression and BRAF analysis in pediatric gliomas

Case #	Site	Diagnosis	OLIG2 score	BRAF	Other
4035	Spinal cord	Pilocytic astrocytoma (WHO I)	3	*K16-B9*	None
2974	Cerebellum	Pilocytic astrocytoma (WHO I)	3	*K16-B11*	None
2085	Cerebellum	Pilocytic astrocytoma (WHO I)	3	*K16-B9*	None
4035	Spinal cord	Pilocytic astrocytoma (WHO I)	3	*K16-B9*	None
2652	Deep grey	Astrocytoma (WHO II)	1	None	None
2995	FTP	Astrocytoma (WHO II)	3	None	None
4282	Cerebellum	Astrocytoma (WHO II)	3	*K16-B9*	None
4825	FTP	Astrocytoma (WHO II)	3	None	None
7269	Deep grey	Astrocytoma, anaplastic (WHO III)	3	None	None
1734	FTP	Astrocytoma, anaplastic (WHO III)	3	V600E	NONE
1762	IV	Astrocytoma, anaplastic (WHO III)	1	None	*TP53*, 273:R>H
7124	FTP	Glioblastoma multiforme	3	None	TP53, 172; V>F, *PIK3C2B/MDM4* (A), *MYC/PVT1*(A)

Surgical site, OLIG2 expression, and results from BRAF analysis in pediatric gliomas are presented. BRAF and KIAA1549 fusions are depicted by the points of exon fusion (e.g., K16-B9 is KIAA1549 exon 16 fused with BRAF exon 9). No statistical difference was noted in OLIG2 score, surgical site, or diagnosis with regards to BRAF mutation. A statistically significant association between IAA-1549-BRAF fusion and the diagnosis of pilocytic astrocytoma was noted

were also OLIG2+ (i.e., (number of OLIG2+ Ki67+ cells)/total Ki67+ cells = 92–94%). However, the mean proportion of OLIG2+ cells that were also Ki67+ (i.e., (number of OLIG2+ Ki67+ cells)/total OLIG2+ cells) varied from 1.0–16.3%. The mean proportion of OLIG2+ cells that were also Ki67+ showed a trend to being associated with increasing tumor grade. As expected, statistical analysis by ANOVA/TukeyHSD test showed the mean proportion of OLIG2+ cells that were also Ki67+ in glioblastoma multiforme WHO IV to be significantly different from pilocytic astrocytoma, astrocytoma WHO II, and anaplastic astrocytoma WHO III ($P = 0.007$, 0.0008, 0.0004, respectively). This finding is in concurrence with data showing a higher Ki67 labeling index in glioblastoma relative to lower grade astrocytomas.

Even though the overall rate of cell proliferation in pilocytic astrocytomas was very low, about 85% of the proliferating cells were also OLIG2+ , which represented only about 1.6 percent of all cells expressing OLIG2. All the ependymoma cases that were OLIG2− showed scattered Ki67 positive nuclei throughout the tissue sections (data not shown). The average percentage of Ki67 + cells that were also OLIG2 + were 84.6% (st. err. = 6.2) for pilocytic astrocytoma, 94.3% (st. err. = 5.7) for grade II astrocytoma, and 92.3% (st. err. = 2.4) for anaplastic astrocytoma WHO grade III. Statistical analysis by ANOVA did not demonstrate any significant difference between astrocytoma groups but did show difference between astrocytoma-ependymoma groups.

BRAF mutation shows no correlation with OLIG2 expressing tumors

Evaluation of *BRAF* mutation status in a subset of pediatric gliomas is presented in Table 5. To test an association between OLIG2 score and *BRAF* mutation, contingency tables were created and analyzed by the Fisher Exact Test. Groups were separated into *BRAF* mutated (which included BRAFV600E missense mutations and *KIAA1549-BRAF* fusion transcripts) and *BRAF* non-mutated. The OLIG2 contingency table separated the patients listed in Table 5 into patients with an OLIG2 score of 3 (*BRAF* mutated $n = 6$, *BRAF* non-mutated $n = 4$), and an OLIG2 score <3 (*BRAF* mutated $n = 0$, *BRAF* non-mutated $n = 2$). No statistically significant association between OLIG2 expression and *BRAF* mutation was determined ($P = 0.45$). Tumor type contingency tables were constructed for pilocytic astrocytoma (*BRAF* mutated $n = 4$, *BRAF* non-mutated $n = 0$), astrocytoma WHO II ((*BRAF* mutated $n = 1$, *BRAF* non-mutated $n = 3$), anaplastic astrocytoma WHO III (*BRAF* mutated $n = 1$, *BRAF* non-mutated $n = 2$), and glioblastoma (*BRAF* mutated n = 0, *BRAF* non-mutated $n = 1$). No statistically significant correlation was identified between the presence of a *BRAF* mutation and tumor diagnosis ($P = 0.11$). However, a statistically significant association between the presence of *KIAA1549-BRAF* fusion transcripts in pilocytic astrocytoma and its absence in the other tumor groups was noted ($P = 0.006$).

Table 6 Top differentially expressed genes in ependymoma and pilocytic astrocytoma

Gene symbol	Ensembl #	logFC	*p*	Probe type
CAM 2	ENSG00000175161	4.90	0.04	_at
FGF12	ENSG00000114279	4.35	0.04	_at
BAI-3	ENSG00000135298	4.18	0.03	_at
SH2	ENSG00000145147	−3.83	0.009	_s_at
Stonin2	ENSG00000140022	−4.24	0.02	_at
RMST	n/a	−6.54	0.02	_at

The most significantly differentially expressed genes between ependymoma and pilocytic astrocytoma as determined by microarray analysis are listed (see "Materials and Methods"). Log fold change (logFC) that is positive denotes genes that are upregulated in pilocytic astrocytoma relative to ependymoma; logFC that is negative denotes genes that were upregulated in ependymoma relative to pilocytic astrocytoma. Affymetrix _at probe types hybridize with one specific transcript whereas _s_at probe types are predicted to hybridize with multiple transcripts of the same gene family. No ensembl id is present for *RMST*, entrez gene id is 196475

RMST rhabdomyosarcoma transcript (non-protein encoding), *FGF12* fibroblast growth factor 12, *SH2* slit homolog 2 *(Drosophila)*

P adjusted *P* value from *lmFit* test using Benferroni correction

In silico analysis of ependymoma and astrocytoma tissue microarray *datasets*

Pilocytic astrocytoma and ependymoma transcriptional expression datasets obtained from previously published Affymetrix expression microarrays were evaluated (see methods). Quality control assessment of the ependymoma and pilocytic astrocytoma datasets demonstrated similar average probe signal intensities and high intergroup correlation (Supplementary Fig. 1). In each group, one of three arrays showed high RNA degradation. Significant differential expression was noted in 1402 of 53272 genes (significance threshold was set to $P < 0.05$ by *t*-test). The genes that were most significantly differentially expressed in the two datasets are listed in Table 6. The *P* value listed is an adjusted *P* value derived after Benferroni correction of the limFit/TopTable *P*-value. Of interest, *SH2* showed significant differential expression with _s_at probes. The _s_at is predicted to bind to more than one transcript of the same gene family, suggesting that gene family members are differentially expressed in these two tumors.

Transcriptional comparison of *OLIG2* genetically null versus wild-type neural stem cells in mice demonstrated differential expression in multiple E-box containing genes [9]. This list of the differentially expressed genes reported by Ligon et al. [9] was used to test for differential expression between the pilocytic astrocytoma and ependymoma microarray data. No statistically significant differential expression of these E-box containing genes was noted when comparing pilocytic astrocytoma and ependymoma array data (in all instances, $P > 0.05$ by *t*-test).

Table 7 lists neural cell lineage associated genes for neural stem cells, astrocytes, oligodendrocytes, and ependymal cells. *SOX2* and *Aquaporin 4* showed significant increased expression in ependymoma relative to pilocytic astrocytoma. Of note, the _s_at probe for *Aquaporin 4* showed no statistically significant difference between the ependymoma and pilocytic astrocytoma datasets ($P = 0.17$), whereas the _at showed significant difference ($P = 0.005$); this suggests that pilocytic astrocytomas may express other genes of a similar family, but do not express the Aquaporin 4 transcript. Relative to ependymomas, pilocytic astrocytomas showed significantly increased expression of *nestin*, *OLIG1*, *OLIG2*, and *Oligodendrocyte Myelin Glycoprotein* (*OMG*). Of note, *PLP1* showed elevated RMA expression measures in pilocytic astrocytoma relative to ependymoma, but the *P* value was slightly above the threshold for significance set for this study ($P = 0.06$). Increased expression of *Rootletin*, a structural protein present in the cilia of ependymal cells [38–40], was significantly higher in ependymoma relative to pilocytic astrocytoma. In contrast to pilocytic astrocytoma, evaluation of the pediatric glioblastoma expression dataset [11] showed minimal expression of *OMG* (mean expression measure = 416.2(81.3)).[1] However, *OLIG2*, *OLIG1*, and *GFAP* were highly expressed in pediatric glioblastoma (mean expression measures 1085.9 (117.1), 2609.4 (426.5), 5499.8 (731), respectively) (see footnote 1).

Discussion

Differential OLIG2 expression in astrocytoma and ependymoma

The transcription factor OLIG2 is expressed in neural progenitor cells and controls replication competence in both neural stem cells and malignant glioma [9]. In addition, OLIG2 expression in a human glioblastoma cell line appeared to down-regulate in vitro cellular motility via RhoA activation [41], suggesting that OLIG2 may regulate various biologic functions in neoplastic glia. Although a majority of the Ki67 immunoreactive cells in pilocytic astrocytomas also expressed OLIG2, most OLIG2 expressing cells were not labeled with Ki67, since pilocytic astrocytomas, as a low grade glioma, typically have a low fraction of proliferating cells. In addition, these tumors have very limited capacity to invade brain parenchyma and tend to uniquely exhibit a circumscribed growth pattern,

[1] Number in parenthesis denotes standard error of the mean of RMA derived expression measures from all pediatric glioblastoma patients.

Table 7 Differential expression of neural lineage genes

Gene name	Genbank #	Diff exp in OLIG2 null (Y/N)	Mean ExpM-EP (st. err.)	Mean ExpM-PA (st. err.)	ExpM-EP/ExpM-PA
Stem cell associated					
SOX2	NM_003106	N	380.23 (13.57)	150.19(34.43)	2.53
Nestin	NM_006617.1	N	254.07 (67.15)	558.29 (96.20)	0.46
BMI1	NMJW5180	Y	957.30 (62.73)	497.97 (90.02)	1.92
Anax6	NM_001155	Y	272.54 (34.65)	486.29 (57.96)	0.56
GFAP	NM_002055	Y	11562.63(160.55)	12983.618(561.08)	0.89
Vimentin	NM_003380	Y	5977.26 (262 44)	6479.32 (2993.85)	0.92
Numb	NM_001005743.1	Y	61.27 (14.7)	46.47 (7.4)	1.3
CCND1	NM_053056.2	N	157.1 (55.68)	165.18(62.7)	0.95
EGFR-1	NM_005228	N	37.9 (3.37)	36.99 (4.37)	1.02
Astrocyte associated					
Aqp4 (probe 1)	NM_001650.4	N	339 93 (33.06)	64.16(110.18)	5.3
Aqp4 (probe 2)	NMJW1650.4	N	3694(1736.48)	310.78 (47.43)	11.89
FGF3	NM_000t42.4	N	11.46(1.24)	10.59(102.42)	11.46
S100b	NM_006272.2	N	2362.04 (858.537)	1827.56(1.72)	1.29
Oligodendrocyte associated					
OLIG1	NM_138983.2	Y	134.82 (14.65)	2271.04 (328)	0.06
OLIG2	NM_Q00533.3	Y	66.88(19.87)	663.45(18.77)	0.1
OMB	NM_138983.2	Y	56.92 (12.4)	545.61 (453.16)	0.1
PDGFRa (probe 1)	NM 006206.4	Y	384.35 (264.4)	34.50(133.47)	1.16
PDGFRa (probe 2)	NM 006206.4	Y	41.2 (16.984	35.4 (3.73)	1.17
MBP (probe 1)	NM_001025081.1	Y	50.87(16.49)	150.01 (9.60)	0.3
MBP (probe 2)	NM_OO1025O81.l	Y	90.57 (34.76)	1431.30 (1332.39)	0.06
PLPI	NM_000533.3	Y	355(125.54)	1455.24 (770.10)	0.24

Genes known to be expressed in the neural stem cell, astrocytic, oligodendroglial, and ependymal lineage are listed. Mean RMA derived expression measures for ependymoma (ExpM-EP) and pilocytic astrocytoma (ExpM-PA). Relative expression of these genes is shown in column (ExpM-EP/ExpM-PA). P = probability calculated by paired two-tailed student's t-test. Diff exp in OLIG null (Y/N) refers to genes that were differentially expressed in OLIG2 null neurospheres compared to wild-type neurospheres as determined by Ligon et al. [9]; Y = differentially expressed, N = not differentially expressed. Affymetrix _at probe types hybridize with one specific transcript whereas _s_at probe types are predicted to hybridize with multiple transcripts of the same gene family

while exhibiting variable motility in the leptomeninges and along white matter tracts. The OLIG2 expressing cells in pilocytic astrocytomas may be a manifestation that these unique astrocytomas arise from certain populations of radial glia or early progenitor cells in common with oligodendroglial lineages [42]. Analyses of both sporadic and NF1-associated pilocytic astrocytomas indicate cell-lineage specific genetic signatures that correspond to regional progenitor cell populations [43]. Comparative analyses of gene expression in sporadic pilocytic astrocytomas demonstrated expression of *SOX10*, *PEN5*, *PLP*, *PMP-22*, *MBP*, and *oligodendroglial myelin glycoprotein*, suggesting that these tumors are uniquely delineated from non-neoplastic white matter and other low grade gliomas, and are more similar to fetal astrocytes and to oligodendroglial lineages [44–46]. Consistent with presence of oligodendroglial progenitors, pilocytic astrocytomas, especially optic nerve tumors, contain significant numbers of O4 immunoreactive cells, and the highest numbers of A2B5 + glial progenitor cells are present in pilocytic astrocytomas of the posterior fossa. An expression analysis of 21 juvenile pilocytic astrocytomas presented additional evidence for the relationship of pilocytic astrocytomas to a population of radial glia or early progenitors. Neurogenesis was one of the major biological processes with detection of 18 deregulated genes with the upregulation of four neurogenesis-related genes in these tumors [47–51]. The marked upregulation of stem cell and oligodendrocyte lineage genes relative to ependymoma determined in the transcriptional microarray data presented in this study is in concordance with previously reported findings.

In all of the diffuse astrocytomas examined, the overwhelming majority of Ki67 positive cells were also OLIG2 positive. This is consistent with OLIG2's role in neural stem cell and glioma cell replication. However, in several examples there were distinct populations of cells that

differentially expressed OLIG2. In one case of glioblastoma (illustrated in Fig. 2, panel D), a subset of polygonal, GFAP negative cells had lost their OLIG2 immunoreactivity, raising the possibility that the OLIG2 positive and negative fractions of tumor cells may have different biological potential and/or function as shown in rodent students [9]. Overall, these data are very similar to OLIG2 data found in adult patients with diffuse astrocytoma [23]. Hence, despite the different molecular signatures and aberrancies between pediatric and adult diffuse astrocytoma, this data suggests that OLIG2 expression in astrocytoma may be conserved between these two age groups.

In comparison to adult gliomas, we found that, with the exception of one case of myxopapillary ependymoma, primary pediatric ependymomas did not significantly express OLIG2. This differential expression of OLIG2 is consistent with the different molecular signatures of adult and pediatric ependymomas [52] and the unique molecular characteristics of pediatric myxopapillary ependymomas [53]. In one case of a recurrent ependymoma, scant OLIG2 immunoreactive cells could be seen, a pattern that is more similar to their adult counterparts [17, 23, 54, 55].

Utility of OLIG2 expression in histopathologic diagnosis of pediatric brain cancers

Our experience with the OLIG2 antibody indicates that this reagent is suitable for routine immunohistochemistry on formalin-fixed, paraffin embedded specimens. We were capable of detecting OLIG2 immunoreactivity in pathology specimens archived for up to 15 years. OLIG2 immunohistochemistry would not be an appropriate marker for distinguishing astrocytomas of different grades. Minimal or the complete absence of nuclear OLIG2 staining in WHO grade II and grade III ependymomas may suggest that in cases where ependymoma and astrocytoma are within the differential diagnosis, OLIG2 immunohistochemistry could aide in distinguishing these two entities. However, the presence of diffuse OLIG2 nuclear staining in one of three myxopapillary ependymomas raises the concern that rare ependymomas may show diffuse OLIG2 nuclear staining. In summary, diffuse OLIG2 nuclear staining in a glial tumor cannot exclude ependymoma from the differential diagnosis.

Acknowledgments The authors wish to thank King Chiu and Michael Wong for expert technical assistance, Cynthia Cowdrey for assistance with case annotations and case archive management, and Mark Segal of the UCSF Clinical and Translational Science Institute Biostatistics core for review of the statistical methodologies. This work was supported by grants from the NIH (D.H.R: (R01NS40511), and grants from the Pediatric Low Grade Glioma Foundation and Pediatric Brain Tumor Foundation. D.H.R. is a Howard Hughes Medical Institute Investigator.

References

1. Pollack IF, Finkelstein SD, Woods J, Burnham J, Holmes EJ, Hamilton RL, Yates AJ, Boyett JM, Finlay JL, Sposto R (2002) Expression of p53 and prognosis in children with malignant gliomas. N Engl J Med 346:420–427
2. C.B.T.R.U.S.: CBTRUS (2008). Statistical report: primary brain tumors in the United States, 2000–2004. Published by the Central Brain Tumor Registry of the United States
3. Bachoo RM, Maher EA, Ligon KL, Sharpless NE, Chan SS, You MJ, Tang Y, DeFrances J, Stover E, Weissleder R, Rowitch DH, Louis DN, DePinho RA (2002) Epidermal growth factor receptor and Ink4a/Arf: convergent mechanisms governing terminal differentiation and transformation along the neural stem cell to astrocyte axis. Cancer Cell 1:269–277
4. Hack MA, Saghatelyan A, de Chevigny A, Pfeifer A, Ashery-Padan R, Lledo PM, Gotz M (2005) Neuronal fate determinants of adult olfactory bulb neurogenesis. Nat Neurosci 8:865–872
5. Menn B, Garcia-Verdugo JM, Yaschine C, Gonzalez-Perez O, Rowitch D, Alvarez-Buylla A (2006) Origin of oligodendrocytes in the subventricular zone of the adult brain. J Neurosci 26:7907–7918
6. Jackson EL, Garcia-Verdugo JM, Gil-Perotin S, Roy M, Quinones-Hinojosa A, VandenBerg S, Alvarez-Buylla A (2006) PDGFR alpha-positive B cells are neural stem cells in the adult SVZ that form glioma-like growths in response to increased PDGF signaling. Neuron 51:187–199
7. Marie Y, Sanson M, Mokhtari K, Leuraud P, Kujas M, Delattre JY, Poirier J, Zalc B, Hoang-Xuan K (2001) OLIG2 as a specific marker of oligodendroglial tumour cells. Lancet 358:298–300
8. Ohnishi A, Sawa H, Tsuda M, Sawamura Y, Itoh T, Iwasaki Y, Nagashima K (2003) Expression of the oligodendroglial lineage-associated markers Olig1 and Olig2 in different types of human gliomas. J Neuropathol Exp Neurol 62:1052–1059
9. Ligon KL, Huillard E, Mehta S, Kesari S, Liu H, Alberta JA, Bachoo RM, Kane M, Louis DN, Depinho RA, Anderson DJ, Stiles CD, Rowitch DH (2007) Olig2-regulated lineage-restricted pathway controls replication competence in neural stem cells and malignant glioma. Neuron 53:503–517
10. Cheng Y, Pang JC, Ng HK, Ding M, Zhang SF, Zheng J, Liu DG, Poon WS (2000) Pilocytic astrocytomas do not show most of the genetic changes commonly seen in diffuse astrocytomas. Histopathology 37:437–444
11. Paugh BS, Qu C, Jones C, Liu Z, Adamowicz-Brice M, Zhang J, Bax DA, Coyle B, Barrow J, Hargrave D, Lowe J, Gajjar A, Zhao W, Broniscer A, Ellison DW, Grundy RG, Baker SJ (2010) Integrated molecular genetic profiling of pediatric high-grade gliomas reveals key differences with the adult disease. J Clin Oncol 28:3061–3068
12. Sung T, Miller DC, Hayes RL, Alonso M, Yee H, Newcomb EW (2000) Preferential inactivation of the p53 tumor suppressor pathway and lack of EGFR amplification distinguish de novo high grade pediatric astrocytomas from de novo adult astrocytomas. Brain Pathol 10:249–259
13. Ohgaki H (2005) Genetic pathways to glioblastomas. Neuropathology 25:1–7
14. Ohgaki H, Kleihues P (2005) Population-based studies on incidence, survival rates, and genetic alterations in astrocytic and oligodendroglial gliomas. J Neuropathol Exp Neurol 64:479–489

15. Ohgaki H, Kleihues P (2005) Epidemiology and etiology of gliomas. Acta Neuropathol 109:93–108
16. Ohgaki H, Kleihues P (2007) Genetic pathways to primary and secondary glioblastoma. Am J Pathol 170:1445–1453
17. Lukashova-v Zangen I, Kneitz S, Monoranu CM, Rutkowski S, Hinkes B, Vince GH, Huang B, Roggendorf W (2007) Ependymoma gene expression profiles associated with histological subtype, proliferation, and patient survival. Acta Neuropathol 113:325–337
18. Balss J, Meyer J, Mueller W, Korshunov A, Hartmann C, von Deimling A (2008) Analysis of the IDH1 codon 132 mutation in brain tumors. Acta Neuropathol 116:597–602
19. Korshunov A, Meyer J, Capper D, Christians A, Remke M, Witt H, Pfister S, von Deimling A, Hartmann C (2009) Combined molecular analysis of BRAF and IDH1 distinguishes pilocytic astrocytoma from diffuse astrocytoma. Acta Neuropathol 118:401–405
20. Sievert AJ, Jackson EM, Gai X, Hakonarson H, Judkins AR, Resnick AC, Sutton LN, Storm PB, Shaikh TH, Biegel JA (2009) Duplication of 7q34 in pediatric low-grade astrocytomas detected by high-density single-nucleotide polymorphism-based genotype arrays results in a novel BRAF fusion gene. Brain Pathol 19:449–458
21. Bar EE, Lin A, Tihan T, Burger PC, Eberhart CG (2008) Frequent gains at chromosome 7q34 involving BRAF in pilocytic astrocytoma. J Neuropathol Exp Neurol 67:878–887
22. Schiffman JD, Hodgson JG, VandenBerg SR, Flaherty P, Polley MY, Yu M, Fisher PG, Rowitch DH, Ford JM, Berger MS, Ji H, Gutmann DH, James CD (2010) Oncogenic BRAF mutation with CDKN2A inactivation is characteristic of a subset of pediatric malignant astrocytomas. Cancer Res 70:512–519
23. Ligon KL, Alberta JA, Kho AT, Weiss J, Kwaan MR, Nutt CL, Louis DN, Stiles CD, Rowitch DH (2004) The oligodendroglial lineage marker OLIG2 is universally expressed in diffuse gliomas. J Neuropathol Exp Neurol 63:499–509
24. Colman H, Giannini C, Huang L, Gonzalez J, Hess K, Bruner J, Fuller G, Langford L, Pelloski C, Aaron J, Burger P, Aldape K (2006) Assessment and prognostic significance of mitotic index using the mitosis marker phospho-histone H3 in low and intermediate-grade infiltrating astrocytomas. Am J Surg Pathol 30:657–664
25. Johnson RA, Wright KD, Poppleton H, Mohankumar KM, Finkelstein D, Pounds SB, Rand V, Leary SE, White E, Eden C, Hogg T, Northcott P, Mack S, Neale G, Wang YD, Coyle B, Atkinson J, DeWire M, Kranenburg TA, Gillespie Y, Allen JC, Merchant T, Boop FA, Sanford RA, Gajjar A, Ellison DW, Taylor MD, Grundy RG, Gilbertson RJ (2010) Cross-species genomics matches driver mutations and cell compartments to model ependymoma. Nature 466:632–636
26. Sharma MK, Mansur DB, Reifenberger G, Perry A, Leonard JR, Aldape KD, Albin MG, Emnett RJ, Loeser S, Watson MA, Nagarajan R, Gutmann DH (2007) Distinct genetic signatures among pilocytic astrocytomas relate to their brain region origin. Cancer Res 67:890–900
27. Gentleman RC, Carey VJ, Bates DM, Bolstad B, Dettling M, Dudoit S, Ellis B, Gautier L, Ge Y, Gentry J, Hornik K, Hothorn T, Huber W, Iacus S, Irizarry R, Leisch F, Li C, Maechler M, Rossini AJ, Sawitzki G, Smith C, Smyth G, Tierney L, Yang JY, Zhang J: Bioconductor: open software development for computational biology and bioinformatics. Genome Biol 5: R80, 2004
28. Bolstad BM, Irizarry RA, Astrand M, Speed TP (2003) A comparison of normalization methods for high density oligonucleotide array data based on variance and bias. Bioinformatics 19:185–193
29. Irizarry RA, Hobbs B, Collin F, Beazer-Barclay YD, Antonellis KJ, Scherf U, Speed TP (2003) Exploration, normalization, and summaries of high density oligonucleotide array probe level data. Biostatistics 4:249–264
30. Irizarry RA, Bolstad BM, Collin F, Cope LM, Hobbs B, Speed TP (2003) Summaries of Affymetrix GeneChip probe level data. Nucleic Acids Res 31:e15
31. Li C, Wong WH (2001) Model-based analysis of oligonucleotide arrays: expression index computation and outlier detection. Proc Natl Acad Sci USA 98:31–36
32. Smyth GK (2004) Linear models and empirical Bayes methods for assessing differential expression in microarray experiments. Stat Appl Genet Mol Biol 3: Article3
33. Huang da W, Sherman BT, Lempicki RA (2009) Systematic and integrative analysis of large gene lists using DAVID bioinformatics resources. Nat Protoc 4:44–57
34. Dennis G Jr, Sherman BT, Hosack DA, Yang J, Gao W, Lane HC, Lempicki RA, David (2003) Database for annotation, visualization, and integrated discovery. Genome Biol 4:P3
35. Preusser M, Budka H, Rossler K, Hainfellner JA (2007) OLIG2 is a useful immunohistochemical marker in differential diagnosis of clear cell primary CNS neoplasms. Histopathology 50:365–370
36. Ishizawa K, Komori T, Shimada S, Hirose T (2008) Olig2 and CD99 are useful negative markers for the diagnosis of brain tumors. Clin Neuropathol 27:118–128
37. Godfraind C (2009) Classification and controversies in pathology of ependymomas. Childs Nerv Syst 25:1185–1193
38. Yang J, Adamian M, Li T (2006) Rootletin interacts with C-Nap1 and may function as a physical linker between the pair of centrioles/basal bodies in cells. Mol Biol Cell 17:1033–1040
39. Yang J, Li T (2006) Focus on molecules: rootletin. Exp Eye Res 83:1–2
40. Yang J, Liu X, Yue G, Adamian M, Bulgakov O, Li T (2002) Rootletin, a novel coiled-coil protein, is a structural component of the ciliary rootlet. J Cell Biol 159:431–440
41. Tabu K, Ohba Y, Suzuki T, Makino Y, Kimura T, Ohnishi A, Sakai M, Watanabe T, Tanaka S, Sawa H (2007) Oligodendrocyte lineage transcription factor 2 inhibits the motility of a human glial tumor cell line by activating RhoA. Mol Cancer Res 5:1099–1109
42. Takei H, Yogeswaren ST, Wong KK, Mehta V, Chintagumpala M, Dauser RC, Lau CC, Adesina AM (2008) Expression of oligodendroglial differentiation markers in pilocytic astrocytomas identifies two clinical subsets and shows a significant correlation with proliferation index and progression free survival. J Neurooncol 86:183–190
43. Sharma MK, Zehnbauer BA, Watson MA, Gutmann DH (2005) RAS pathway activation and an oncogenic RAS mutation in sporadic pilocytic astrocytoma. Neurology 65:1335–1336
44. Bannykh SI, Stolt CC, Kim J, Perry A, Wegner M (2006) Oligodendroglial-specific transcriptional factor SOX10 is ubiquitously expressed in human gliomas. J Neurooncol 76:115–127
45. Colin C, Baeza N, Bartoli C, Fina F, Eudes N, Nanni I, Martin PM, Ouafik L, Figarella-Branger D (2006) Identification of genes differentially expressed in glioblastoma versus pilocytic astrocytoma using Suppression Subtractive Hybridization. Oncogene 25:2818–2826
46. Gutmann DH, Hedrick NM, Li J, Nagarajan R, Perry A, Watson MA (2002) Comparative gene expression profile analysis of neurofibromatosis 1-associated and sporadic pilocytic astrocytomas. Cancer Res 62:2085–2091
47. Wong KK, Chang YM, Tsang YT, Perlaky L, Su J, Adesina A, Armstrong DL, Bhattacharjee M, Dauser R, Blaney SM, Chintagumpala M, Lau CC (2005) Expression analysis of juvenile pilocytic astrocytomas by oligonucleotide microarray reveals two potential subgroups. Cancer Res 65:76–84
48. Buffo A, Vosko MR, Erturk D, Hamann GF, Jucker M, Rowitch D, Gotz M (2005) Expression pattern of the transcription factor

Olig2 in response to brain injuries: implications for neuronal repair. Proc Natl Acad Sci USA 102:18183–18188
49. Chen Y, Miles DK, Hoang T, Shi J, Hurlock E, Kernie SG, Lu QR (2008) The basic helix-loop-helix transcription factor olig2 is critical for reactive astrocyte proliferation after cortical injury. J Neurosci 28:10983–10989
50. Goldman JE, Corbin E (1988) Isolation of a major protein component of Rosenthal fibers. Am J Pathol 130:569–578
51. Quinlan RA, Brenner M, Goldman JE, Messing A (2007) GFAP and its role in Alexander disease. Exp Cell Res 313:2077–2087
52. Kilday JP, Rahman R, Dyer S, Ridley L, Lowe J, Coyle B, Grundy R (2009) Pediatric ependymoma: biological perspectives. Mol Cancer Res 7:765–786
53. Barton VN, Donson AM, Kleinschmidt-Demasters BK, Birks DK, Handler MH, Foreman NK (2009) Unique molecular characteristics of pediatric myxopapillary ependymoma. Brain Pathol 20:560–570
54. Tamiolakis D, Papadopoulos N, Venizelos I, Lambropoulou M, Nikolaidou S, Bolioti S, Kiziridou A, Manavis J, Alexiadis G, Simopoulos C (2006) Loss of chromosome 1 in myxopapillary ependymoma suggests a region out of chromosome 22 as critical for tumour biology: a FISH analysis of four cases on touch imprint smears. Cytopathology 17:199–204
55. Gilhuis HJ, van der Laak J, Wesseling P, Boerman RH, Beute G, Teepen JL, Grotenhuis JA, Kappelle AC (2004) Inverse correlation between genetic aberrations and malignancy grade in ependymal tumors: a paradox? J Neurooncol 66:111–116